Structural basis for the function and regulation of the receptor protein tyrosine phosphatase CD45

Hyun-Joo Nam,[1,2] Florence Poy,[1] Haruo Saito,[1,2,3] and Christin A. Frederick[1,2]

[1]Dana-Farber Cancer Institute, Boston, MA 02115
[2]Department of Biological Chemistry and Molecular Pharmacology, Harvard Medical School, Boston, MA 02115
[3]Institute of Medical Science, the University of Tokyo, Tokyo 108-8639, Japan

CD45 is the prototypic member of transmembrane receptor–like protein tyrosine phosphatases (RPTPs) and has essential roles in immune functions. The cytoplasmic region of CD45, like many other RPTPs, contains two homologous protein tyrosine phosphatase domains, active domain 1 (D1) and catalytically impaired domain 2 (D2). Here, we report crystal structure of the cytoplasmic D1D2 segment of human CD45 in native and phosphotyrosyl peptide–bound forms. The tertiary structures of D1 and D2 are very similar, but doubly phosphorylated CD3ζ immunoreceptor tyrosine–based activation motif peptide binds only the D1 active site. The D2 "active site" deviates from the other active sites significantly to the extent that excludes any possibility of catalytic activity. The relative orientation of D1 and D2 is very similar to that observed in leukocyte common antigen–related protein with both active sites in an open conformation and is restrained through an extensive network of hydrophobic interactions, hydrogen bonds, and salt bridges. This crystal structure is incompatible with the wedge model previously suggested for CD45 regulation.

CORRESPONDENCE
Haruo Saito:
h-saito@ims.u-tokyo.ac.jp

Abbreviations used: BNL, Brookhaven National Laboratory; D1, domain 1; D2, domain 2; ITAM, immunoreceptor tyrosine-based activation motif; LAR, leukocyte common antigen–related; PTP, protein tyrosine phosphatase; RPTP, receptor-like PTP; R_{sym}, R factor for symmetry-related reflections; Sel-Met, selenomethionine.

Protein tyrosine phosphorylation is a key mechanism for nearly every aspect of cell regulation, ranging from cell survival and proliferation to apoptotic cell death in multicellular eukaryotes. Tyrosine phosphorylation itself is regulated by a concerted action of protein tyrosine kinases and protein tyrosine phosphatases (PTPs). The human genome encodes as many as 38 classical PTPs, which share highly homologous PTP domains (1). These PTPs are divided into two major subfamilies: 17 nonreceptor (or cytoplasmic) PTPs and 21 receptor-like (transmembrane) PTPs. CD45, also known as the leukocyte common antigen, is the prototype of the receptor-like PTP (RPTP) subfamily and is found in all nucleated hematopoietic cells (2–4). CD45 is essential for development and antigen-induced activation of T and B cells (5–9). Mutations in the human CD45 gene have been associated with SCID and multiple sclerosis (10–12). CD45 controls immune response, both positively and negatively, by dephosphorylating a number of signaling molecules, including Src family kinases (Lck and Fyn), the CD3ζ chain of TCR, and ZAP-70 kinase (13, 14).

H.-J. Nam's present address is Dept. of Biochemistry and Molecular Biology, University of Florida, Gainesville, FL 32610.

Like many other RPTPs, CD45 consists of an extracellular receptor-like region, a short transmembrane segment, and a cytoplasmic region comprising tandem PTP domains (see Fig. 1 A). The length of the extracellular segment varies among the CD45 isoforms generated by alternative splicing (15). Mutational analyses have shown that the membrane proximal PTP domain 1 (D1), but not the membrane distal domain 2 (D2), is catalytically active (16). The entire cytoplasmic region of CD45 is conserved among vertebrates, from shark to mammalian (17). The strong conservation of the CD45 D2 primary structure implies a functional role, but this role is not yet clearly defined. Nonetheless, there are observations that suggest a regulatory role of the catalytically inert D2 domain (18). D2 perhaps influences the activity of D1 by direct intermolecular and intramolecular interaction, as shown by in vitro binding studies (19, 20). Phosphorylation of D2 by casein kinase 2 enhances the phosphatase activity of D1, consistent with a regulatory role of the D2 domain (21). It was also reported that the CD45 D2 domain could, by itself, bind one of the important substrates, Lck, facilitating its dephosphorylation by D1

domain (22). In the case of another RPTP, leukocyte common antigen–related (LAR) protein, we observed a high degree of similarity between the crystal structures of the D1 and D2 domains (23). Perhaps consistent with the structural similarity of D2 and D1, only two amino acid substitutions were required to convert the otherwise inert D2 domains of LAR and PTPα into active enzymes (23–25). These findings led us to propose that D2 might function as an auxiliary catalytic site that would be activated under specific cellular conditions or in the presence of a proper substrate (23).

A generalized model, known as the dimeric inhibition model or the wedge hypothesis, for the regulation of RPTP activity has been proposed based on the crystal structure of the RPTPα D1 domain (26). The RPTPα D1 domain formed a homodimeric structure in the crystal, in which the active site of one monomer was blocked by an NH_2-terminal helix-turn-helix wedge motif of the other monomer, suggesting that dimer formation on the membrane negatively regulates the PTP activity. Experimental data that seem to corroborate this model have been reported. For example, ligand-induced dimerization of the epidermal growth factor receptor–CD45 chimeric molecule and enforced covalent dimerization of full-length PTPα resulted in down-regulation of their PTP activities (27, 28). Impairment of dimer formation, by introducing mutations into the wedge region, led to apparent PTP activation both in vivo and in vitro (28–30). Transiently expressed PTPα was shown to exist predominantly as homodimers (31). In the same study, however, mutations in the wedge region reduced but did not completely abolish PTPα dimerization, suggesting that other factors are also contributing to the dimer formation.

Here, we report crystal structures of the CD45 cytoplasmic region containing both the D1 and D2 domains. We also determined crystal structures of the CD45 cytoplasmic region bound to phosphopeptide substrates; one bound to a nonspecific short phosphopeptide, and the other bound to the membrane-proximal immunoreceptor tyrosine-based activation motifs (ITAMs) of the CD3ζ chain. We will describe the key features of CD45 and its substrate interactions and discuss the implications of these structures as they impact on our understanding of the mechanism of D1 and the potential function of D2. In these structures, CD45 exists as a monomer with the D1 active site cleft, as well as the D2 site, clearly unobstructed by the rest of the protein chain. The observed intramolecular orientation of the D1 and D2 domains precludes the formation of a dimer of the type predicted by the dimeric inhibition model. Such a D1 dimer interaction is impossible because of significant steric hindrance generated from the overlap of the attached D2 domains.

RESULTS

Overview of the CD45 D1D2 structure determination

In human leukocytes, various CD45 isoforms of different lengths are expressed by combinatorial alternative splicing (15). All isoforms, however, share the exactly identical cytoplasmic region of 707 amino acids, which is composed of a

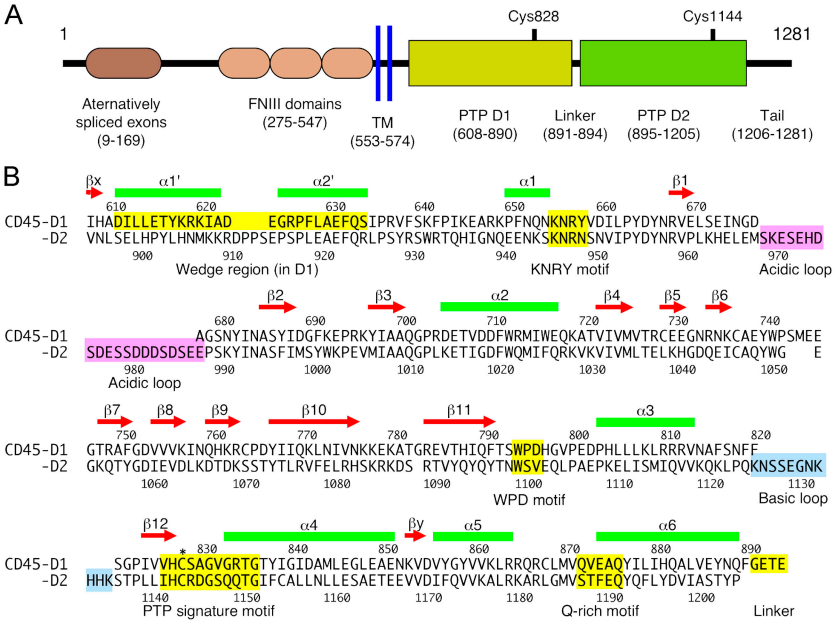

Figure 1. The overall structure of the CD45 molecule and the amino acid sequence of the CD45 D1D2 domains. (A) A schematic model of the human CD45 molecule. Numbers in parentheses are amino acid positions. In this work, we refer to the amino acid positions as they appear in the mature protein of the longest isoform (reference 15). FNIII domain, fibronectin III–like domain. (B) The segment of the CD45 cytoplasmic region whose structure is described here is shown as primary sequence. The D1 and D2 sequences are aligned according to their secondary structures. The secondary structure elements are represented as green bars for α helices and red arrows for β strands on top of the amino acid sequence. The wedge region, the KNRY motif, the WPD motif, the PTP signature motif, the Q-rich motif, and the interdomain linker region are marked by yellow overlay. The acidic and basic loops are marked by magenta and blue overlays, respectively.

juxtamembrane spacer segment, the PTP D1 domain, a short interdomain linker, the PTP D2 domain, and a COOH-terminal tail (Fig. 1 A). In this report, we will refer to the amino acid positions as they appear in the mature protein of the longest isoform (15). According to this convention, the cytoplasmic domain is from 575 to 1281, and the catalytic site cysteine residues are at 828 (Cys828) in D1 and at 1144 (Cys1144) in D2, respectively. An alignment of the D1 and D2 sequences, as well as several key features in the PTP domain, are shown in Fig. 1 B. Previously, we and others have shown that the CD45 D2 PTP domain has no catalytic activity (16, 32), whereas others reported different findings (33). Later in this report, we will present the structural basis of why the CD45 D2 domain cannot have a catalytic activity. For convenience sake, however, we will use terms such as "D2 active site," "D2 catalytic site," etc., to refer to the region in D2 that corresponds in PTP domain structure to the D1 active site, without implying an actual catalytic activity.

To obtain the materials for crystallographic studies, the CD45 cytoplasmic region containing both the D1 and D2 domain was expressed in *Escherichia coli* as six-His–tagged proteins and purified to apparent homogeneity. In our initial attempts where we used the entire cytoplasmic region of CD45, we could not obtain sufficiently good crystals. This was likely due to the presence of an extended COOH-terminal segment that seems flexible. To circumvent this problem, we generated a series of CD45 cytoplasmic fragments, differing both at the NH_2- and COOH-terminal positions, to obtain the optimal domain boundaries for crystallization. Thus, we obtained two different crystals, CD45 D1D2 (597–1213) with Cys828 to Ser (C828S) mutation, and wild-type CD45 D1D2 (603–1203), which gave optimal diffraction data. In addition, a number of datasets were analyzed from crystals grown in the presence of different ions (sulfate, phosphate, and tungstate ions), monomeric phosphotyrosine, and two different phosphotyrosyl-peptides.

The best quality data have been collected from monoclinic crystals of selenomethionine (Sel-Met)–substituted CD45-D1D2 (597–1213) (C828S) protein with phosphotyrosine-containing peptides (derived from polyoma middle T antigen and CD3ζ ITAM motif; see below for more details). The crystal structures for both complexes were solved to 2.9 Å resolution by the molecular replacement method. Data collection and the final refinement statistics for these complexes are summarized in Table I. Both datasets are of similar quality with respect to resolution and agreement of R factor for symmetry-related reflections (R_{sym}). The corresponding protein structures demonstrate correct geometric parameters as well as the desired lack of model bias. The current CD45 model includes 589 residues (601–1205), excluding the disordered acidic loop segment of D2.

In Fig. 2, the structure of the CD45 cytoplasmic region is viewed from three directions. For comparison, the structure of LAR D1D2, the only other RPTP for which the tandem PTP domain structure has been solved (23), is reproduced in the inset as viewed from the same direction as the CD45 structure shown at the top left. It is clear that the observed orientation of the D1 and D2 domains in CD45 is very similar to that adopted by LAR. It also can be seen that the overall structures of the D1 and D2 domains are essentially identical to each other. Both D1 and D2 domains consists of a highly twisted nine-stranded mixed β sheet flanked

Table I. Crystallographic data and refinement statistics

	CD45 D1D2 C828S and phosphopeptide complexes	
	Polyoma middle T antigen	CD3 ζITAM-1
Crystallographic data		
Space group	P2(1)	P2(1)
Cell parameters	a = 86.9 Å, b = 57.9 Å, c = 159.3 Å, β = 98.78	a = 86.0 Å, b 5 59.7 Å, c = 160.5 Å, β 5 99.58
Z	4	4
X-ray source	X12, BNL	X12, BNL
Resolution	30–2.9 Å	30–2.9 Å
Observations (*n*)	99,669	99,514
Unique reflections (complete)	32,025 (93.0%)	29,466 (81.5%)
R_{sym}[a]	0.079	0.071
Refinement statistics of current model		
Resolution	30–2.9 Å	30–2.9 Å
Protein atoms (*n*)	9,457	9,416
Substrate atoms (*n*)	74	122
R_{cryst} (work[b]/free[c])	0.263/0.306	0.258/0.315
Rmsd bond lengths	0.010 Å	0.010 Å
Rmsd bond angles	1.59°	1.57°

[a]$R_{sym} = \Sigma_h \Sigma_i |I_{ih} - \langle I_h \rangle| / \Sigma_h \Sigma_i \langle I_h \rangle$, where $\langle I_h \rangle$ is the mean of the observations I_{ih} of reflection h.
[b]$R_{working} = \Sigma ||F_{obs}| - |F_{calc}|| / \Sigma |F_{obs}|$.
[c]R_{free} = R factor for a selected subset (5%) of the reflections that was not included in prior refinement calculations.

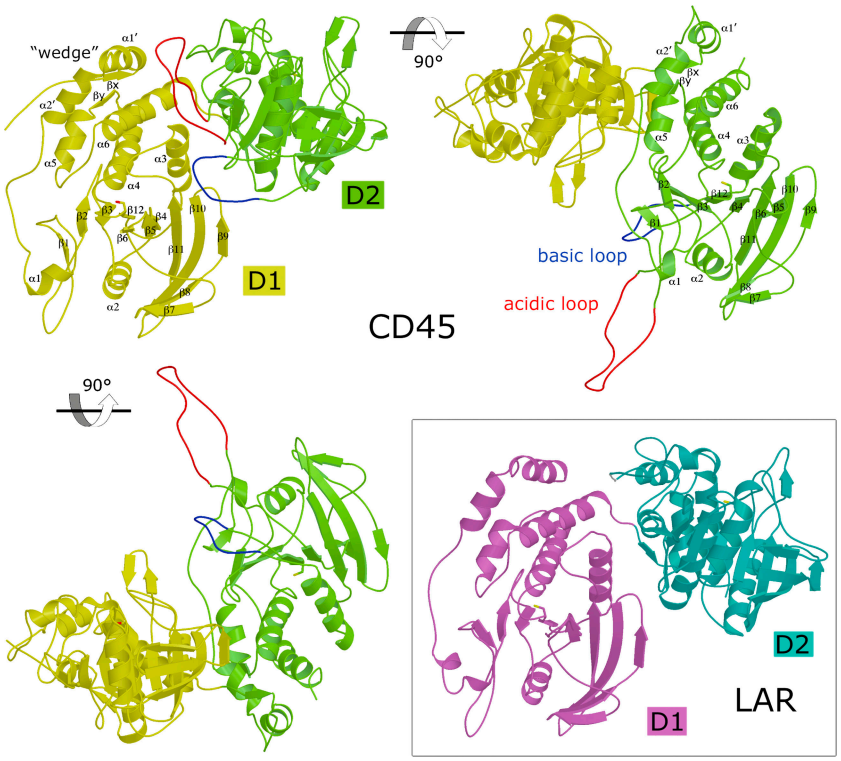

Figure 2. Ribbon diagram representations of the CD45 D1D2 domains. Three different views are shown of the CD45 structure. The D1 and D2 domains are shown in yellow and green, respectively. On the top left, the viewer is looking straight into the D1 active site, and the corresponding active site of D2 is facing upward (y direction). For comparison, a corresponding diagram of LAR D1D2 is shown in the boxed inset. Two additional views of CD45 molecule are generated by rotating the molecule by 90° along the horizontal axis in both directions (top right and bottom left). The secondary structure elements in D1 and D2 are labeled, respectively, in the top left and top right panels. The acidic and basic loops are shown in magenta and blue, respectively. The wedge region is also shown.

by four α helices on one side and two α helices on the other. In general, this domain structure is similar to those of previously reported PTPs (26, 34, 35). Secondary structure elements in D1 and D2, as determined in our structure, are shown in Fig. 1 B.

Interaction of phosphopeptides at the D1 active site

To understand the mechanisms of substrate recognition and dephosphorylation by CD45, purified CD45 D1D2 (597–1213) C828S was crystallized in the presence of either phosphotyrosine (i.e., monomeric amino acid) or one of two different phosphopeptides. C828S mutant was used to prevent dephosphorylation of the substrates.

The first phosphopeptide (QQQQNQLpYNELNLGRREEpYDVLDKRRG, where pY is phosphotyrosine) is the membrane proximal ITAM of the CD3ζ chain (ζITAM-1) with both the tyrosine residues phosphorylated. CD3ζ is an important CD45 substrate and contains three ITAMs in its cytoplasmic domain. An ITAM is defined as a 20–25–amino acid sequence containing two YxxL/I segments separated by six to eight amino acid residues (36). Each of the three ITAMs in CD3ζ is tyrosine phosphorylated when TCR is activated. The doubly phosphorylated ITAMs serve as docking sites for the tandem SH2-containing ZAP-70, which initiates a cascade of signal transduction events (37, 38). It has been demonstrated that CD3ζ and CD45 physically associate in vivo and that CD45 efficiently dephosphorylates CD3ζ in vitro (39, 40). Mutational analyses of the tyrosine residues in the membrane-proximal ITAM of CD3ζ have shown that the two YxxL segments in the ITAM are functionally distinct (41), indicating the critical importance of regulating ITAM phosphorylation states.

The second phosphopeptide (NPTpYS) is derived from the polyoma middle T antigen. Although this peptide is probably not a physiologically meaningful substrate of CD45, it has the advantage of being a well-known short phospho-substrate.

When CD45 was crystallized in the presence of monomeric phosphotyrosine, there was a well-defined density corresponding to this moiety in the D1 active site pocket, but no comparable density in the D2 domain that would suggest the presence of phosphotyrosine (not depicted). In the crystal structure of the CD45 D1D2 complexed with ζITAM-1, although there are two phosphotyrosyl residues in ζITAM-1, assignable extra densities were visible only at the D1 active site. No extra densities are discernible at the D2 active site, or in fact anywhere else associated with the protein. Electron densities for six amino acids surrounding the second phosphotyrosyl residue (REEpYDV) are visible at the D1 active site (Fig. 3, A and B). This result appears consistent with the

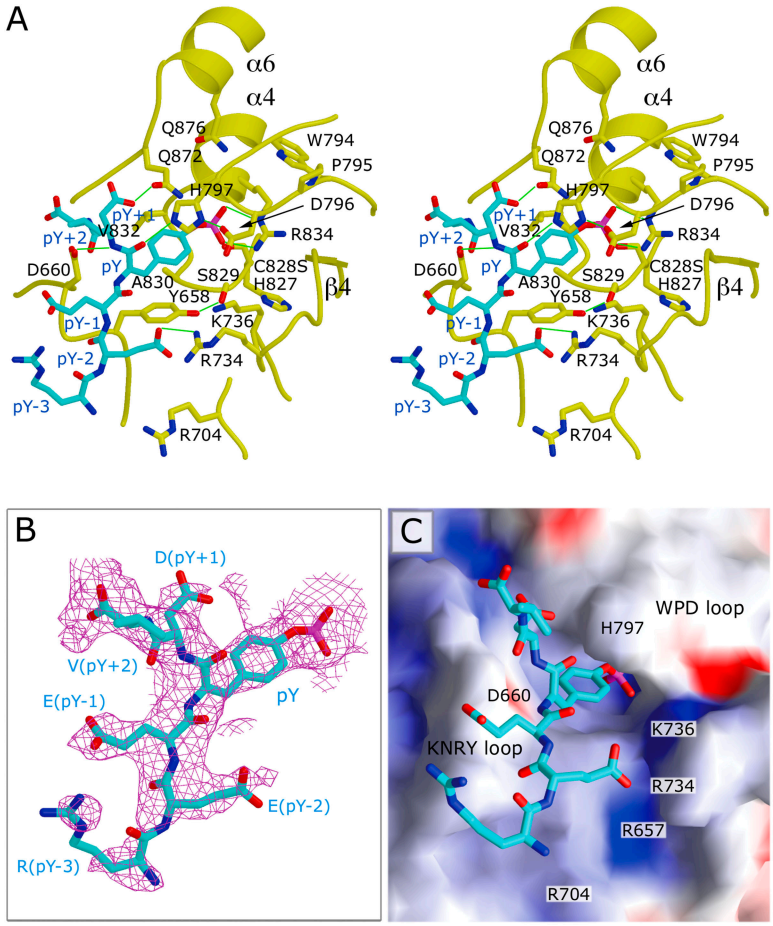

Figure 3. Structure of the CD45 D1D2 bound to the CD3 ζITAM-1 phosphopeptide. (A) A stereo view of the D1 active site with the CD3 ζITAM-1 phosphopeptide. Relevant hydrogen bonds between the side chains of the CD45 protein and the ITAM-1 peptide are shown by green lines. (B) The phosphopeptide model is shown with a $2|F_{obs}|-|F_{calc}|$ composite omit map at the 0.9 σ contour level. (C) Molecular surface representation of the D1 active site bound to the CD3 ζITAM-1 peptide. The surfaces are colored according to the electrostatic potential: blue for positive and red for negative. The peptide model is shown using a ball and stick representation.

previous in vitro analyses showing that the CD45 phosphatase prefers the second phosphotyrosine in ζITAM-1 over the first phosphotyrosine (42). Similarly, in the structure of CD45 bound with the polyoma phosphopeptide (NPTpYS), electron density corresponding to four residues (PTpYS) was visible only at the D1 active site (Fig. 4, A and B).

For both the ζITAM-1 peptide and the polyoma peptide, the general features of the phosphotyrosine binding to the CD45 D1 active site are similar. The active site pocket of CD45 D1 is composed of a base formed by the residues of the PTP signature motif, surrounded by three additional segments: the KNRY motif, the WPD motif, and the Q-rich motif (Fig. 1 B). Extensive hydrogen bonding occurs between the phosphotyrosyl residue and the active site pocket. Within the PTP signature motif, the active site Cys828 (Ser in our structure) is positioned for nucleophilic reaction with the substrate phosphorus. Hydrogen bonds are observed between the phosphoryl moiety and the main chain amide groups of the PTP signature motif, as well as the basic side chain of Arg834. The tyrosine residue of the phosphopeptide is stabilized by aromatic ring stacking with Tyr658 in the KNRY motif. The WPD motif, which contains catalytically important Asp796, adopts an open conformation when crystallized with sulfate ions. This loop, however, shows a closed conformation in all of our substrate-bound structures. The imidazole ring of His797 makes hydrophobic contact with the phenyl ring of the substrate phosphotyrosyl residue as well as a hydrogen bond with the backbone carbonyl group of the phosphotyrosyl residue. The acidic side chain of Asp660 in the KNRY loop is making a hydrogen bond with the amide group of the pY+1 residue. This positioning of the two residues of opposite charges (His797 and Asp660) seems to determine the backbone configuration of the substrate phosphotyrosyl residue and residues COOH-terminal to it. The conserved Gln872 and Gln876 residues in the Q-rich motif are positioned surrounding the active site to generate the required charge distribution and pocket shape that accommodate a phosphate leaving group during catalysis. Overall, most interactions between the substrate phosphotyrosyl residue and the D1 active site are similar to those seen in the substrate-bound complexes of PTP1B and *Yersinia* PTP (43, 44), with the exception of the one between the

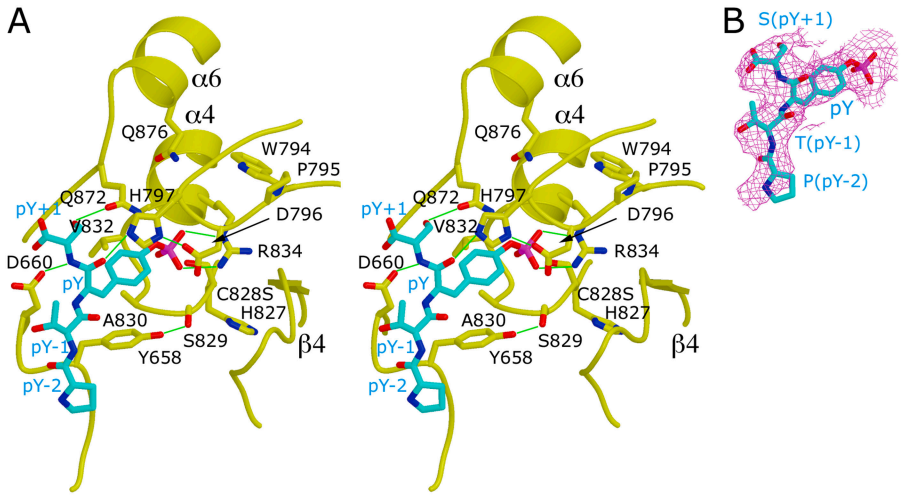

Figure 4. Structure of the CD45 D1D2 bound to NPTpYS. (A) A stereo view of the D1 active site with the NPTpYS peptide. Relevant hydrogen bonds between the side chains of the CD45 protein and the NPTpYS peptide are shown by green lines. (B) The phosphopeptide model is shown with a $2|F_{obs}|-|F_{calc}|$composite omit map at the 0.9 σ contour level.

carbonyl of the phosphotyrosyl residue and the basic side chain of His797. The residue corresponding to His797 is a phenylalanine in PTP1B. In the CD45 structure, His797 may add extra interactions and strengthen the binding of the substrate phosphotyrosyl residue.

Fig. 3 A shows detailed interactions between six amino acids (REEpYDV) of the ζITAM-1 substrate and the CD45 protein. On the NH_2-terminal side of the phosphotyrosyl residue, the Glu (pY-1) side chain is pointing in the direction opposite that of the phosphotyrosine. The Glu (pY-1) side chain is exposed to solvent without any interaction with the protein; thus, the presence of a hydrophilic residue at this position might be favored for binding. The carboxyl group of the Glu (pY-2) makes a hydrogen bond contact with the guanidium group of Arg734. The surface charge distribution of the CD45 protein at this region shows an extended positively charged surface contributed by residues Arg657, Arg704, Arg734, and Lys736 (Fig. 3, A and C). The negatively charged Glu (pY-2) fits nicely into this positively charged pocket and seems to be important for binding to the CD45 PTP. The positive charges of the protein at this region may repel the basic side chain of Arg (pY-3), thus allowing no direct interactions with the protein.

On the COOH-terminal side of ζITAM-1, the Asp (pY+1) side chain points toward the CD45 protein and makes a hydrogen bond with the side chain of Gln872. The main chain backbone of the Val (pY+2) runs almost perpendicular to the rest of the peptides. The overall extent of these contacts between the ζITAM-1 substrate and the D1 domain is consistent with the previous results from PTP1B–substrate complexes (43), indicating that residues between pY-3 and pY+2 of the substrate determine phosphatase specificities.

In the structure of CD45 bound with the polyoma phosphopeptide (NPTpYS), electron densities corresponding to four residues (PTpYS) are visible at the D1 active site (Fig. 4). In addition to the interactions between the phosphotyrosine moiety and the protein, the NH_2-terminal peptide residues make contact with the KNRY loop. Thr (pY-1) is in van der Waals contact with the side chain of Asp660, and the ring of Pro (pY-2) is making a van der Waals contact with the Tyr658 ring. The terminal oxygen of Ser (pY+1) is hydrogen bonded with the side chain of residue Gln872 in the Q-rich motif.

Based on these structures, we propose that the optimal interaction of CD45 active site and phosphotyrosyl substrate occurs when a hydrophilic residue occupies the pY-1 position and negatively charged amino acids are located around the pY-2 position. The Lck and Fyn protein tyrosine kinases, two of the best known CD45 substrates, fit into these criteria. These protein kinases have two tyrosine phosphorylation sites: one in their activation loops (DENEpYTAR in Lck and EDNEpYTAR in Fyn) and another near their COOH termini (TEGQpYQPQ in Lck and TEPQpYQPG in Fyn). All of these peptides contain hydrophilic residues at the pY-1 position, as in the ζITAM-1 sequence. In the activation loop peptides, the acidic amino acid at pY-3 (and perhaps at pY-4) is likely to interact with the positively charged pocket of CD45. In the COOH-terminal peptides, we can more confidently speculate that the negatively charged Glu (pY-3) interacts with the positively charged pocket of CD45, because the residues at the Y-2 position, namely Gly and Pro, are optimal at generating conformations to accommodate such interactions. The NH_2-terminal phosphorylation site of ζITAM-1 (NQLpYNE) lacks these criteria. The presence of the hydrophobic Leu residue at the pY-1 position, and lack of any negatively charged amino acids at the pY-2 and pY-3 positions, explain the reduced affinity of the NH_2-terminal phosphorylation site for the CD45 PTP.

The CD45 D2 domain is a totally inactive phosphatase

The strong structural conservation of the CD45 D2 domain implies that it serves a cellular function, but it is still of ma-

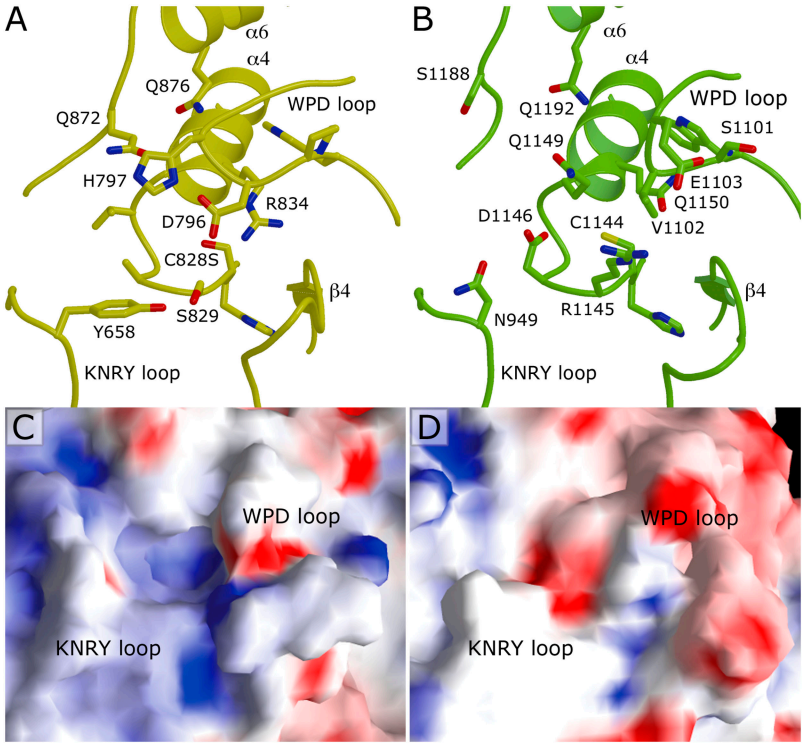

Figure 5. Comparisons between the D1 and D2 catalytic centers. (A and B) Ribbon diagrams of active sites in D1 (A) and D2 (B). Side chains of residues implicated in catalysis are shown. (C and D) Molecular surface of the active sites of D1 (C) and D2 (D), as seen from the same direction as in A and B. The surfaces are colored as in Fig. 3 C. Due to the closed conformation of the WPD loop in our structure, the surface charge distribution of the D1 active site pocket could not be easily viewed. To help show a comparison, the WPD loop of the D1 active site is presented in a partially open conformation in this figure, as was seen in the D2 active site.

jor mystery. Our CD45 structure suggests that the function of the CD45 D2 domain is very different from its LAR counterpart. In the LAR D1D2 structure we determined previously, the inactive D2 domain maintains an active site topology similar to that of D1. With only two substitutions of the key residues in the surrounding loops, LAR D2 could be converted to a very active enzyme (23). In contrast, the PTP signature motif in CD45 D2 deviates from the consensus sequence to the extent that it can no longer accommodate a phosphoryl group (VHCSAGVGRTG in D1 vs. IHCRDGSQQTG in D2). As a result, the CD45 D2 domain has a significantly reduced number of available ligands for oxygen binding, a significantly altered shape of the active site pocket, as well as a reduced accessibility of the Cys nucleophile. Fig. 5, A and B, show the details of the D1 and D2 active sites, respectively. In catalytically active PTP structures, including the CD45 D1 domain, the side chain of the highly conserved Arg in the PTP motif makes two hydrogen bonds with the phosphoryl group and is very important for both substrate binding and transition state stabilization (43). The fatal substitution of this Arg to Gln in CD45 D2 (Gln1150) results in a shorter side chain that is unable to interact with a phosphoryl group in the same manner as Arg834 in D1. In addition, as shown in Fig. 5 B, the bulky side chains of Asp1146 and Gln1149 are protruding toward what would have been the phosphoryl group binding site. The Nδ1 of Asp1146 is also making a hydrogen bond with a backbone amide group, blocking the potential binding partner of the phosphoryl group. Finally, the presence of the negative charge at Asp1146, together with the lack of a positively charged amino acid at 1150, must repel any incoming phosphoryl group. Thus, it is apparent that the deviations from the consensus at three positions (Asp1146, Gln1149, and Gln1150) will abolish any affinity for an incoming phosphoryl group. Indeed, despite a significant molar excess of the potential small molecule substrates present in the crystallization trials, there is no evidence of their presence in any of the CD45 D2 domains in any of the crystal forms obtained.

The structure of the loops surrounding the D2 active site is also quite different from that of the D1 active site. This can be easily visualized by the surface representation of the active sites with their respective charge distributions (Fig. 5, C and D). The WPD loop in D2 shows a partially open conformation, and the invariant Asp, which acts as general acid/base in active PTPs, is substituted with Val1102 in D2. This substitution will certainly impair catalytic activity. The KNRY loop also shows a quite different conformation in D2. The conserved Tyr involved in the stabilizing π–π interactions with the phenyl ring of the ligand phosphotyrosyl residue is replaced by Asn949 in D2, further contributing to the reduced affinity for phosphotyrosyl substrates. In conclusion, the CD45 D2 structure does not have even the remotest possibility of retaining a cata-

lytic activity. This represents a clear mechanistic distinction between CD45 and other RPTPs, even as compared with its close relative, LAR.

Possible role of the CD45 D2 domain deduced from its structure

Inspection of the D2 structure, as detailed in this section, suggests that it has a role in substrate recruitment. The CD45 D2 domain has two unique features that are not found in any other PTPs, including LAR. Those are the two extra loops, referred to, respectively, as the acidic and basic loops, whose positions are shown in Fig. 2 by color. The 20–amino acid acidic loop (SKESEHDSDESSDDDSDSEE [969–988]), located between the β1 and β2 strands, is mostly disordered and flexible. Although not all of the residues in the acidic loops could be seen in the crystal structure, the location and approximate model can be visualized based on the rest of the structure and the electron density observed in this area. The 11–amino acid basic loop (KNSSEGNKHHK [1126–1136]) is located between the α3 helix and the β12 strand. The entire basic loop could be refined in one of the two molecules in the P2(1) space group, but the temperature factor for these residues is quite high (average main chain B factor is ∼20 Å^2 higher than the rest of the molecule), reflecting the flexible nature of the basic loop.

It has been reported that deletion of the acidic loop, or substitution of four Ser residues to Ala in the acidic loop, diminished CD3-mediated activation of T lymphocytes (45). Furthermore, phosphorylation of Ser residues in the acidic loop by casein kinase 2 is important for CD45 functions (21). Our structure lends a mechanistic explanation to such observations. Both the acidic and basic loops in D2 are located on the same side of the surface of the molecule with respect to the D1 active site. Because both loops have significant charge biases and are located very close to the active site in D1, they could easily serve as initial substrate recruiting sites. When phosphorylated, these loops may undergo a conformational change or induce a change in the catalytic site to facilitate docking of incoming substrates.

Extensive interaction between the D1 and D2 domains

In this work, we obtained crystals of CD45-D1D2, without peptide, in two different space groups: P2(1) and P6(3)22. Although the crystallographic contacts between the neighboring molecules are totally different in the two crystal forms, the intramolecular spatial relationship between the D1 and D2 domains is essentially identical in both crystal forms. Several cocrystals of CD45-D1D2 with phosphopeptides also had very similar D1–D2 domain orientation. If the atoms of the D1 domains from two different crystal forms, P2(1) and P6(3)22, are superimposed, the atoms in the D2 domains differ by an average (root-mean-square) distance of 3.2 Å between the equivalent Cα atoms. They differ by 2.9 Å between the two noncrystallographically related molecules in the P2(1) space group. The average distances are even smaller between the residues located at the interface of the D1 and D2 domains (∼1.5 Å). In all cases, the D1 and D2 domains are connected by a four-residue linker, GETE (891–894), and packed tightly against each other. This linking segment is conserved between CD45 and LAR (GETE and GHTE, respectively) and is bound to both D1 and D2 domains in a similar fashion in the two different proteins. The interdomain orientation between D1 and D2 is further stabilized by an extensive network of interactions, consisting of hydrogen bonds, van der Waals interactions, and salt bridges (Fig. 6). Hydrophobic interactions were observed at two regions of the interdomain surface. Phe890 at the end of D1 α6 is making van der Waals contact with the Phe1173 in D2 α5, and Pro765 (in the loop between β9 and β10 of D1) is in contact with Tyr1001 and Trp1002 (in the loop be-

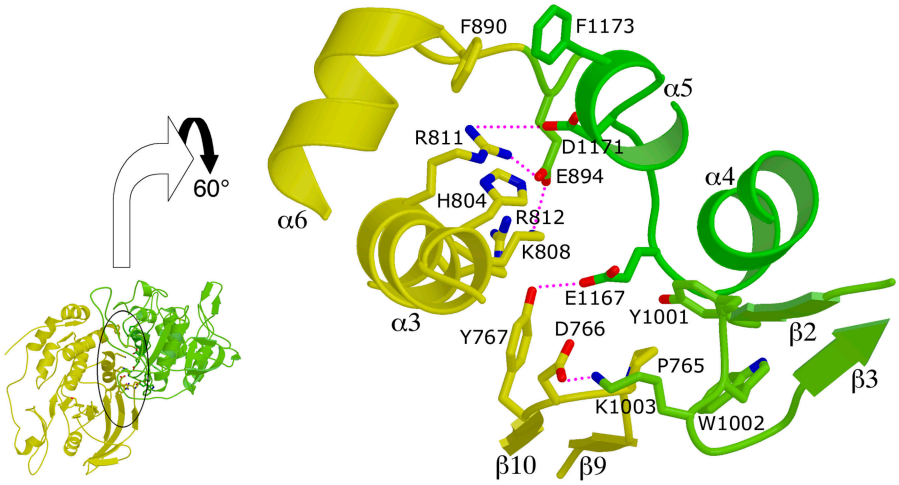

Figure 6. Intramolecular interactions between the D1 and D2 domains. The circled region of the small diagram on the left shows the interface between the D1 (yellow) and D2 (green) domains. The detailed view of this area, rotated 60°, along the horizontal axis is shown on the right. Amino acid residues involved in interdomain interactions are shown with carbon in yellow, oxygen in red, and nitrogen in blue. Selected hydrogen bonds are shown by red dotted lines.

tween β2 and β3 of D2). Hydrophobic interactions are further stabilized by salt bridges, observed between the basic side chains (His804, Lys808, Arg811, and Arg812) in D1 α3 and acidic side chains (Glu1167 and Asp1171) in the D2 domain. Among these residues, Arg811 and Arg812 are highly conserved among most RPTP D1 domains, and Glu1167 and Asp1171 are conserved in most RPTP D2 domains. Overall, there are extensively complementary surfaces between the D1 and D2 domains, including the residues of the α3 and α6 helices of D1 and the α4 and α5 helices of D2.

These results suggest that the intramolecular D1–D2 orientation reported here is a likely state of the CD45 molecule in the cell. Furthermore, this relative orientation of the D1 and D2 domains of CD45 is very similar to that of LAR, which we reported previously (23), suggesting that this is typical of most, if not all, two-domain RPTPs. The energy required to separate D1 from D2 is ~16 kcal/mol, which is probably sufficient to keep the two domains bound together even if they are not tethered by the linker. This conclusion is consistent with the earlier observations, based on fluorescence resonance energy transfer and coprecipitation analyses, which showed strong intermolecular and intramolecular interactions between D1 and D2 domains of various RPTP proteins (46, 47). Nonetheless, it should be noted that the extracellular domain and transmembrane segment, which are not included in our structure, may have a significant influence on the conformation of D1–D2 orientation in cells.

Because of these extensive D1–D2 interactions, even subtle structural changes in D2 might affect the D1 conformation. Indeed, a mutation in D2 is known (Q1180G in mouse CD45, which is equivalent to Q1192G in our human structure) that nearly completely abolishes the D1 catalytic activity (48). Because Gln1192 is not making any direct contact with D1 residues, its effect must be propagated indirectly through the D1–D2 interface. Exactly how this is effected will require the structural solution of the CD45 Q1192G mutant protein. Thus, stabilization of the D1 domain seems an important role of D2. We can hypothesize that the primordial two-domain RPTPs had two enzymatically active PTP domains, and over the history of RPTP evolution, D1 and D2 domains established extensive association to the extent that one requires another for maintenance of its proper structure. Thus, although the CD45 D2 domain has lost its catalytic activity, it may still be needed to support the D1 structure and activity.

DISCUSSION

An outstanding question concerning RPTPs is how extracellular stimuli, such as ligand binding, may affect the catalytic activity of the cytoplasmic PTP domains. A major model concerning this question was proposed based on the crystal structure of the RPTPα D1 domain that crystallized as a dimer (26). In the RPTPα dimer structure, the active site in each monomer was blocked by the NH_2-terminal α1′-turn-α2′ segment (called "wedge") of an opposing monomer, thus preventing substrate access to the active site. It was further suggested that ligand-induced dimerization inactivates the RPTP phosphatase activity. The wedge hypothesis is aesthetically attractive because, if proven, it would depict RPTPs as a perfect mirror image of receptor tyrosine kinases, where ligand-induced dimerization typically activates the kinases. This hypothesis was apparently supported by in vivo and in vitro analyses of RPTPα and epidermal growth factor receptor–CD45 chimeric molecules (28–30).

Nonetheless, our present CD45 structure shows that the cytoplasmic region of CD45 does not dimerize even when highly concentrated, and the dimeric interaction as observed for RPTPα D1 would be impossible given the D1–D2 intramolecular domain orientation. The CD45 D1–D2 interaction seems too tight to allow the deformation needed for D1–D1 interaction, given the extensive interface and the essentially identical D1–D2 orientation observed among different CD45 crystal forms and LAR. Furthermore, the CD45 wedge region (610–634; refer to Fig. 2) is not involved in any intermolecular interaction. We previously reached a similar conclusion regarding lack of dimerization of the D1D2 domains based on the LAR structure (23). At that time, we could not know for sure whether what we observed for LAR represented a general phenomenon or merely an isolated case of that particular RPTP. However, now that we have solved the CD45 structure itself, we can convincingly conclude that the steric hindrance from the D2 domain prevents D1–D1 dimer formation in CD45 as proposed previously (26).

Our data, therefore, indicate that the regulation of CD45 cannot be simply explained by the dimeric inhibition model mediated by the NH_2-terminal wedge. Nonetheless, the wedge region (helix-turn-helix motif) is conserved, suggesting that it has a regulatory function (29, 30). If so, however, it is likely that the wedge region influences the CD45 function by a mechanism other than the dimer formation. Indeed, it was recently shown that CD45 could dimerize without the cytoplasmic domain (49). Furthermore, a CD45 wedge mutation that had significant effect on the CD45 function did not affect the dimerization. Obviously, more studies, including the structures of additional RPTPs as well as the extracellular portion of CD45, will be needed to further such understanding.

MATERIALS AND METHODS

Nomenclature. An individual amino acid is indicated by the standard three-letter or one-letter code, followed by its amino acid position. Thus, both Cys828 and C828 represent the cysteine at position 828. Missense mutations are designated by the one-letter code. C828S, for example, indicates the mutation of Cys828 to serine. Peptide sequences are indicated by the one-letter amino acid code. pY is a phospho-tyrosine residue. pY-1 indicates the amino acid position immediately on the NH_2-terminal side of pY, and pY+2 represents the second amino acid from pY on the COOH-terminal side.

Preparation of recombinant proteins. Proteins were expressed using the T7 expression system essentially as described previously (23, 50). The catalytic site mutant (C828S) of CD45-D1D2 (597–1213) was tagged at the NH_2 terminus with cleavable six-His, whereas the wild-type CD45-D1D2

(603–1203) was tagged with noncleavable COOH-terminal six-His. The proteins were first purified using a Ni-affinity column (and in the case of the cleavable tag, six-His was removed by the TEV protease). The proteins were further purified using an anion exchange column. After desalting, the proteins were concentrated to 10 mg/ml. For expression of Sel-Met–substituted protein, the methionine auxotrophic strain *E. coli* B834 (DE3) was used. The transformed cells were grown in the M9 medium supplemented with 40 mg/ml L–Sel-Met and 19 other amino acids. Purification was performed following the similar procedure as the native protein.

Crystallization. Two different crystal forms of CD45 D1D2 protein were obtained. Monoclinic crystals of CD45-D1D2 (597–1213) C828S were grown by vapor diffusion in hanging drops in 100 mM sodium acetate, pH 5.0, 10–13% (wt/vol) polyethylene glycol (PEG) 4000, 10 mM dithiothreitol (DTT), and 25% glycerol, with various additives such as ammonium sulfate, phosphotyrosine, or phosphopeptide. For cocrystallization experiments with phosphopeptides, either NPTpYS derived from polyoma middle T antigen or QQQQNQLpYNELNLGRREEpYDVLDKRRG, the membrane proximal ITAM of the CD3ζ chain (ζITAM-1), was added to the purified CD45-D1D2 (597–1213) (C828S) protein so that the final concentration of the peptides would be ~10 mM.

Hexagonal crystals of CD45-D1D2 (603–1203) with noncleavable COOH-terminal six-His tag were grown by vapor diffusion in hanging drops in 100 mM MOPS/NaOH, pH 6.5, 13–15% (wt/vol) PEG 8000, 0.5 M ammonium sulfate, 10 mM DTT, and 15% glycerol.

X-ray data collection. Crystals were flash-frozen with the crystallization solution. Diffraction data were collected at various synchrotron sources including the F1 station of the Cornell High Energy Synchrotron Source, the SBC-CAT of Advanced Photon Source in Argonne National Laboratory, and the X12 station of Brookhaven National Laboratory (BNL). Images were processed with DENZO, and data were scaled and processed with SCALEPACK (51).

Structure determination. Initially, the structure of CD45-D1D2 (597–1213) C828S bound with sulfate ion was determined. In this crystal form, two molecules were expected in an asymmetric unit. The structure was determined by molecular replacement using an unaltered model of the D2 domain of RPTP LAR as a search model with the program AmoRe (52). An initial search revealed four unambiguous positions of phosphatase domains. After rigid body refinement, the identity of the PTP domains was determined based on the locations of the N and COOH termini, and amino acid sequence was changed to reflect the CD45 molecule. Several iterative cycles of refinement were performed using minimization and anisotropic temperature factor refinement options of the crystallography & NMR system (CNS) software packages, followed by manual rebuilding (53). Noncrystallographic symmetry restraints were used throughout refinement. Composite omit map in CNS was used for most of the refinement steps.

A refined model of the CD45-D1D2 (597–1213) C828S–sulfate complex was then used to determine other crystal structures. A Sel-Met dataset was collected with the intention of confirming the refined structure. Because of the anisomorphism, the Sel-Met data could not be used for phase determination. Instead, an F_{obs}-F_{calc} map was generated using the CD45-D1D2 (597–1213) C828S model and Sel-Met data. The map showed strong (>3.5σ) corresponding densities at most of the Met positions, validating the structure. For structure determination of Sel-Met CD45-D1D2 (597–1213) C828S–phosphopeptide complexes, a refined model of Sel-Met CD45-D1D2 (597–1213) C828S was used to generate an F_{obs}-F_{calc} map. For both phosphopeptides, ζITAM-1 and polyoma middle T antigen, initial maps revealed clear peptide density at each D1 active site. Refinement procedures include minimization and individual temperature factor refinement using the CNS software package.

In the hexagonal crystal of CD45-D1D2 (603–1203), one molecule was expected in an asymmetric unit. For the structure determination, the refined model of the CD45-D1D2 (597–1213) C828S was used for molecular replacement. The CD45 D1 and D2 domains were used either together or separately for the search. In both cases, the highest solutions were the same, and the relative orientation of the D1 and D2 domains was basically identical as in monoclinic crystals.

Calculation of the free energy required to separate the D1 and D2 domains. Environment-free energies of the CD45 D1D2 proteins have been calculated using the program ENVIRON (54). The atomic model of the protein was manually modified so that there were no interdomain interactions between the D1 and D2 domains, with the linker region still attached. The environment-free energies of the several modified models were calculated, and the energy required for separation of the D1 and D2 domains was calculated by subtracting the free energy of the native protein from that of the modified proteins.

Coordinates of the CD45/CD3 ζITAM-1 and the CD45/polyoma middle T antigen complex have been deposited into the Protein Data Bank with the ID clones IYGR and IYGU, respectively.

Graphics. Molecular models were generated using the programs ALSCRIPT (55), MOLSCRIPT (56), RASTER3D (57), BOBSCRIPT (56, 58), and GRASP (59).

We thank J. Wang, H. Song, J. Augustine, and K. Tan for help with synchrotron data collection; M. Eck for the Polyoma middle T antigen peptide; and Cornell High Energy Synchrotron Source, Argonne National Laboratory, and BNL operators for technical support.

This work was supported in part by a grant from National Institutes of Health (NIH; R01-GM53415) to H. Saito and C.A. Frederick and Grants-in-Aid for Scientific Research from the Ministry of Education, Culture, Sports, Science and Technology of Japan to H. Saito. H.-J. Nam was a recipient of an NIH training grant (T32-CA09361).

The authors have no conflicting financial interests.

Submitted: 13 September 2004
Accepted: 3 December 2004

REFERENCES

1. Alonso, A., J. Sasin, N. Bottini, I. Friedberg, I. Friedberg, A. Osterman, A. Godzik, T. Hunter, J. Dixon, and T. Mustelin. 2004. Protein tyrosine phosphatases in the human genome. *Cell*. 117:699–711.
2. Tonks, N.K., H. Charbonneau, C.D. Diltz, E.H. Fischer, and K.A. Walsh. 1988. Demonstration that the leukocyte common antigen CD45 is a protein tyrosine phosphatase. *Biochemistry*. 27:8695–8701.
3. Trowbridge, I.S., and M.L. Thomas. 1994. CD45: an emerging role as a protein tyrosine phosphatase required for lymphocyte activation and development. *Annu. Rev. Immunol*. 12:85–116.
4. Hermiston, M.L., Z. Xu, and A. Weiss. 2003. CD45: a critical regulator of signaling thresholds in immune cells. *Annu. Rev. Immunol*. 21: 107–137.
5. Pingel, J.T., and M.L. Thomas. 1989. Evidence that the leukocyte common antigen is required for antigen-induced T lymphocyte proliferation. *Cell*. 58:1055–1065.
6. Koretzky, G.A., J. Picus, M.L. Thomas, and A. Weiss. 1990. Tyrosine phosphatase CD45 is essential for coupling T-cell antigen receptor to the phosphatidyl inositol pathway. *Nature*. 346:66–68.
7. Koretzky, G.A., J. Picus, T. Schultz, and A. Weiss. 1991. Tyrosine phosphatase CD45 is required for T-cell antigen receptor and CD2-medicated activation of a protein tyrosine kinase and interleukin 2 production. *Proc. Natl. Acad. Sci. USA*. 88:2037–2041.
8. Justement, L.B., K.S. Campbell, N.C. Chien, and J.C. Cambier. 1991. Regulation of B cell antigen receptor signal transduction and phosphorylation by CD45. *Science*. 252:1839–1842.
9. Kishihara, K., J. Penninger, V.A. Wallace, T.M. Kundig, K. Kawai, A. Wakeham, E. Timms, K. Pfeffer, P.S. Ohashi, M.L. Thomas, et al. 1993. Normal B lymphocyte development but impaired T cell maturation in CD45-exon 6 protein tyrosine phosphatase-deficient mice. *Cell*. 74:143–156.
10. Jacobsen, M., D. Schweer, A. Ziegler, R. Gaber, S. Schock, R.

Schwinzer, K. Wonigeit, R. Lindert, O. Kantarci, J. Schaefer-Klein, et al. 2000. A point mutation in PTPRC is associated with the development of multiple sclerosis. *Nat. Genet.* 26:495–499.
11. Kung, C., J.T. Pingel, M. Heikinheimo, T. Klemola, K. Varkila, L.I. Yoo, K. Vuopala, M. Poyhonen, M. Uhari, M. Rogers, et al. 2000. Mutations in the tyrosine phosphatase CD45 gene in a child with severe combined immunodeficiency disease. *Nat. Med.* 6:343–345.
12. Tchilian, E.Z., D.L. Wallace, R.S. Wells, D.R. Flower, G. Morgan, and P.C.L. Beverley. 2001. A deletion in the gene encoding the CD45 antigen in a patient with SCID. *J. Immunol.* 166:1308–1313.
13. Mustelin, T., K.M. Coggeshall, and A. Altman. 1989. Rapid activation of the T-cell tyrosine protein kinase pp56*lck* by the CD45 phosphotyrosine phosphatase. *Proc. Natl. Acad. Sci. USA.* 86:6302–6306.
14. Desai, D.M., J. Sap, O. Silvennoinen, J. Schlessinger, and A. Weiss. 1994. The catalytic activity of the CD45 membrane-proximal phosphatase domain is required for TCR signaling and regulation. *EMBO J.* 13:4002–4010.
15. Streuli, M., L.R. Hall, Y. Saga, S.F. Schlossman, and H. Saito. 1987. Differential usage of three exons generates at least five different mRNAs encoding human leukocyte common antigens. *J. Exp. Med.* 166:1548–1566.
16. Streuli, M., N.X. Krueger, T. Thai, M. Tang, and H. Saito. 1990. Distinct functional roles of the two intracellular phosphatase like domains of the receptor-linked protein tyrosine phosphatases LCA and LAR. *EMBO J.* 9:2399–2407.
17. Okumura, M., R.J. Matthews, B. Robb, G.W. Litman, P. Bork, and M.L. Thomas. 1996. Comparison of CD45 extracellular domain sequences from divergent vertebrate species suggests the conservation of three fibronectin type III domains. *J. Immunol.* 157:1569–1575.
18. Kashio, N., W. Matsumoto, S. Parker, and D.M. Rothstein. 1998. The second domain of the CD45 protein tyrosine phosphatase is critical for interleukin-2 secretion and substrate recruitment of TCR-ζ in vivo. *J. Biol. Chem.* 50:33856–33863.
19. Felberg, J., and P. Johnson. 1998. Characterization of recombinant CD45 cytoplasmic domain proteins: evidence for intramolecular and intermolecular interactions. *J. Biol. Chem.* 273:17839–17845.
20. Felberg, J., and P. Johnson. 2000. Stable interdomain interaction within the cytoplasmic domain of CD45 increases enzyme stability. *Biochem. Biophys. Res. Commun.* 271:292–298.
21. Wang, Y., W. Guo, L. Liang, and W.J. Esselman. 1999. Phosphorylation of CD45 by casein kinase 2: modulation of activity and mutational analysis. *J. Biol. Chem.* 274:7454–7461.
22. Felberg, J., D.C. Lefebvre, M. Lam, Y. Wang, D.H.W. Ng, D. Birkenhead, J.L. Cross, and P. Johnson. 2004. Subdomain X of the kinase domain of Lck binds CD45 and facilitates dephosphorylation. *J. Biol. Chem.* 279:3455–3462.
23. Nam, H.-J., F. Poy, N.X. Krueger, H. Saito, and C.A. Frederick. 1999. Crystal structure of the tandem phosphatase domains of RPTP LAR. *Cell.* 97:521–530.
24. Lim, K.L., P.R. Kolatkar, K.P. Ng, C.H. Ng, and C.J. Pallen. 1998. Interconversion of the kinetic identities of the tandem catalytic domains of receptor-like protein tyrosine phosphatase PTPα by two point mutations is synergistic and substrate-dependent. *J. Biol. Chem.* 273:28986–28993.
25. Buist, A., Y.-L. Zhang, Y.-F. Keng, L. Wu, Z.-Y. Zhang, and J. den Hertog. 1999. Restoration of protein-tyrosine phosphatase activity into the membrane-distal domain of receptor protein-tyrosine phosphatase α. *Biochemistry.* 38:914–922.
26. Bilwes, A.M., J. den Hertog, T. Hunter, and J.P. Noel. 1996. Structural basis for inhibition of receptor protein-tyrosine phosphatase-alpha by dimerization. *Nature.* 382:555–559.
27. Desai, D.M., J. Sap, J. Schlessinger, and A. Weiss. 1993. Ligand-mediated negative regulation of a chimeric transmembrane receptor tyrosine phosphatase. *Cell.* 73:541–554.
28. Jiang, G., J. den Hertog, J. Su, J. Noel, J. Sap, and T. Hunter. 1999. Dimerization inhibits the activity of receptor-like protein-tyrosine phosphatase-α. *Nature.* 401:606–610.
29. Majeti, R., A.M. Bilwes, J.P. Noel, T. Hunter, and A. Weiss. 1998. Dimerization-induced inhibition of receptor protein tyrosine phosphatase function through an inhibitory wedge. *Science.* 279:88–91.
30. Majeti, R., Z. Xu, T.G. Parslow, J.L. Olson, D.I. Daikh, N. Killeen, and A. Weiss. 2000. An inactivating point mutation in the inhibitory wedge of CD45 causes lymphoproliferation and autoimmunity. *Cell.* 103:1059–1070.
31. Jiang, G., J. den Hertog, and T. Hunter. 2000. Receptor-like protein tyrosine phosphatase alpha homodimerizes on the cell surface. *Mol. Cell. Biol.* 20:5917–5929.
32. Johnson, P., H.L. Ostergaard, C. Wasden, and I.S. Trowbridge. 1992. Mutational analysis of CD45: a leukocyte-specific protein tyrosine phosphatase. *J. Biol. Chem.* 267:8035–8041.
33. Tan, X., D.R. Stover, and K.A. Walsh. 1993. Demonstration of protein tyrosine phosphatase activity in the second of two homologous domains of CD45. *J. Biol. Chem.* 268:6835–6838.
34. Barford, D., A.J. Flint, and N.K. Tonks. 1994. Crystal structure of human protein tyrosine phosphatase 1B. *Science.* 263:1397–1404.
35. Hoffmann, K.M.V., N.K. Tonks, and D. Barford. 1997. The crystal structure of domain 1 of receptor protein-tyrosine phosphatase μ. *J. Biol. Chem.* 272:27505–27508.
36. Samelson, L.E., and R.D. Klausner. 1992. Tyrosine kinases and tyrosine-based activation motifs: current research on activation via the T cell antigen receptor. *J. Biol. Chem.* 267:24913–24916.
37. Chan, A.C., M. Iwashima, C.W. Turck, and A. Weiss. 1992. ZAP-70: a 70 kd protien-tyrosine kinase that associates with the TCR ζ chain. *Cell.* 71:649–662.
38. Gauen, L.K., Y. Zhu, F. Letourneur, Q. Hu, J.B. Bolen, L.A. Matis, R.D. Klausner, and A.S. Shaw. 1994. Interactions of p59fyn and ZAP-70 with T-cell receptor activation motifs: defining the nature of a signalling motif. *Mol. Cell. Biol.* 14:3729–3741.
39. Volarevic, S., C.M. Burns, J.J. Sussman, and J.D. Ashwell. 1990. Intimate association of Thy-1 and the T-cell antigen receptor with the CD45 tyrosine phosphatase. *Proc. Natl. Acad. Sci. USA.* 87:7085–7089.
40. Furukawa, T., M. Itoh, N.X. Krueger, M. Streuli, and H. Saito. 1994. Specific interaction of the CD45 protein-tyrosine phosphatase with tyrosine-phosphorylated CD3 ζ chain. *Proc. Natl. Acad. Sci. USA.* 91: 10928–10932.
41. Sunder-Plassmann, R., F. Lialios, M. Madsen, S. Koyasu, and E.L. Reinherz. 1997. Functional analysis of immunoreceptor tyrosine-based activation motif (ITAM)-mediated signal transduction: the two YxxL segments within a single CD3zeta-ITAM are functionally distinct. *Eur. J. Immunol.* 27:2001–2009.
42. Hegedûs, Z., V. Chitu, G.K. Tóth, C. Finta, G. Váradi, I. Andó, and W. Monostori. 1999. Contribution of kinases and the CD45 phosphatase to the generation of tyrosine phosphorylation patterns in the T-cell receptor complex ζ chain. *Immunol. Lett.* 67:31–39.
43. Jia, Z., D. Barford, A.J. Flint, and N.K. Tonks. 1995. Structural basis for phosphotyrosine peptide recognition by protein tyrosine phosphatase 1B. *Science.* 268:1754–1758.
44. Phan, J., K. Lee, S. Cherry, J.E. Tropea, T.R.J. Burke, and D.S. Waugh. 2003. High-resolution structure of the *Yersinia pestis* protein tyrosine phosphatase YopH in complex with a phosphotyrosyl mimetic-containing hexapeptide. *Biochemistry.* 42:13113–13121.
45. Greer, S.F., Y. Wang, C. Raman, and L.B. Justement. 2001. CD45 function is regulated by an acidic 19-amino acid insert in domain II that serves as a binding and phosphoacceptor site for casein kinase 2. *J. Immunol.* 166:7208–7218.
46. Blanchetot, C., L.G.J. Tertoolen, and J. den Hertog. 2002. Regulation of receptor protein-tyrosine phosphatase alpha by oxidative stress. *EMBO J.* 21:493–503.
47. Blanchetot, C., L.G. Tertoolen, J. Overvoorde, and J. den Hertog. 2002. Intra- and intermolecular interactions between intracellular domains of receptor protein-tyrosine phosphatases. *J. Biol. Chem.* 277: 47263–47269.
48. Ng, D.H.W., A. Maiti, and P. Johnson. 1995. Point mutation in the second phosphatase domain of CD45 abrogates tyrosine phosphatase activity. *Biochem. Biophys. Res. Commun.* 206:302–309.
49. Xu, Z., and A. Weiss. 2002. Negative regulation of CD45 by differen-

tial homodimerization of the alternatively spliced isoforms. *Nat. Immunol.* 3:764–771.
50. Itoh, M., M. Streuli, N.X. Krueger, and H. Saito. 1992. Purification and characterization of the catalytic domains of the human receptor-linked protein tyrosine phosphatases HPTPβ, leukocyte common antigen (LCA), and leukocyte common antigen-related molecule (LAR). *J. Biol. Chem.* 267:12356–12363.
51. Otwinowski, Z. 1993. Oscillation data reduction program. *In* Data Collection and Processing: Proceedings of the CCP4 Study Weekend. L. Sawyer, N. Isaac, and S. Baily, editors. SERC Daresbury Laboratory, Warrington, UK. 55–62.
52. Navaza, J. 1994. AmoRe: an automated package for molecular replacement. *Acta Crystallogr. A.* 50:157–163.
53. Brünger, A.T., P.D. Adams, G.M. Clore, W.L. DeLano, P. Gros, R.W. Grosse-Kunstleve, J.-S. Jiang, J. Kuszewski, M. Nilges, N.S. Pannu, et al. 1998. Crystallography & NMR system: A new software suite for macromolecular structure determination. *Acta Crystallogr. D. Biol. Crystallogr.* 54:905–921.
54. Koehl, P., and M. Delarue. 1994. Polar and nonpolar atomic environments in the proteins core: implications for folding and binding. *Proteins.* 20:264–278.
55. Barton, G.J. 1993. ALSCRIPT: a tool to format multiple sequence alignments. *Protein Eng.* 6:37–40.
56. Kraulis, P.J. 1991. MOLSCRIPT: a program to produce both detailed and schematic plots of protein structures. *J. Appl. Crystallogr.* 24:946–950.
57. Merritt, E.A., and D.J. Bacon. 1997. Raster3D: photorealistic molecular graphics. *Methods Enzymol.* 277:505–524.
58. Esnouf, R.M. 1997. An extensively modified version of MolScript that includes greatly enhanced coloring capabilities. *J. Mol. Graph.* 15:132–134.
59. Nicholls, A., K. Sharp, and B. Honig. 1991. Protein folding and association: insights from the interfacial and thermodynamic properties of hydrocarbons. *Proteins.* 11:281–296.